Soft Matter

Accepted Manuscript

This is an *Accepted Manuscript*, which has been through the Royal Society of Chemistry peer review process and has been accepted for publication.

Accepted Manuscripts are published online shortly after acceptance, before technical editing, formatting and proof reading. Using this free service, authors can make their results available to the community, in citable form, before we publish the edited article. We will replace this *Accepted Manuscript* with the edited and formatted *Advance Article* as soon as it is available.

You can find more information about *Accepted Manuscripts* in the Information for Authors.

Please note that technical editing may introduce minor changes to the text and/or graphics, which may alter content. The journal's standard Terms & Conditions and the Ethical guidelines still apply. In no event shall the Royal Society of Chemistry be held responsible for any errors or omissions in this *Accepted Manuscript* or any consequences arising from the use of any information it contains.

ROYAL SOCIETY OF CHEMISTRY

www.rsc.org/softmatter

Graphical and textual abstract for the contents pages

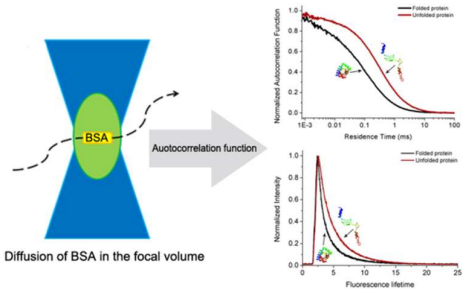

The structural transition of bovine serum albumin (BSA) leads to significant changes in the diffusion coefficients and fluorescence lifetimes of ATTO-BSA.

Soft Matter Accepted Manuscript

Cite this: DOI: 10.1039/c0xx00000x

www.rsc.org/xxxxxx

ARTICLE TYPE

Tracking Structural Transitions of Bovine Serum Albumin in Surfactant Solutions by Fluorescence Correlation Spectroscopy and Fluorescence Lifetime Analysis

Xuzhu Zhang, Andrzej Poniewierski, Sen Hou, Krzysztof Sozański, Agnieszka Wiśniewska, Stefan Wieczorek, Tomasz Kalwarczyk, Lili Sun, Robert Hołyst*

Received (in XXX, XXX) Xth XXXXXXXXX 20XX, Accepted Xth XXXXXXXXX 20XX
DOI: 10.1039/b000000x

The structural dynamics of proteins is crucial to their biological functions. A precise and convenient method to determine the structural changes of a protein is still urgently needed. Herein, we employ fluorescence correlation spectroscopy (FCS) to track the structural transition of bovine serum albumin (BSA) in low concentrated cationic (cetyltrimethylammonium chloride, CTAC), anionic (sodium dodecyl sulfate, SDS), and nonionic (pentaethylene glycol monododecyl ether, $C_{12}E_5$ and octaethylene glycol monododecyl ether, $C_{12}E_8$) surfactant solutions. BSA is labelled with the fluorescence dye called ATTO-488 (ATTO-BSA) to obtain steady fluorescence signals for measurements. We find that the diffusion coefficient of BSA decreases abruptly with the surfactant concentration in ionic surfactant solutions at concentrations below the critical micelle concentration (CMC), while it is constant in nonionic surfactant solutions. According to the Stokes-Sutherland-Einstein equation, the hydrodynamic radius of BSA in ionic surfactant solutions amounts to ~6.5 nm, which is 1.7 times larger than in pure water or in nonionic surfactant solutions (3.9 nm). The interaction between BSA and ionic surfactant monomers is believed to cause the structural transition of BSA. We confirm this proposal by observing a sudden shift of the fluorescence lifetime of ATTO-BSA, from 2.3 ns to ~3.0 ns, in ionic surfactant solutions at the concentration below CMC. No change in the fluorescence lifetime is detected in nonionic surfactant solutions. Moreover, by using FCS we are also able to identify whether the structural change of protein results from its self-aggregation or unfolding.

Introduction

The understanding of structural changes of proteins in different media is an important issue in biochemistry and biophysics. Previous studies on the interaction between proteins and surfactants by varieties of methods, such as circular dichroism spectroscopy,[1] NMR,[2, 3] light scattering,[4] small angle X-ray scattering (SAXS)[5, 6] and small angle neutron scattering (SANS),[7] partially revealed the conformational changes of proteins in surfactant solutions.[8, 9] Results obtained from these techniques consistently show that ionic surfactants interact strongly with proteins and cause the formation of protein-surfactant complexes. Guo et al[10] summarized several models proposed to describe the interaction. Among them, the "necklace-bead" model, proposed by Takagi[11] and tested by Turro and Lei,[2] gained the strongest support and acceptance by other researchers.[4, 12, 13] However, at present we still do not completely understand how the structure of a protein changes quantitatively in different charged surfactant solutions on the basis of the classical "necklace-bead" model. The structural dynamics is usually subtle and difficult to probe by traditional ensemble experiments.[14]

Fluorescence correlation spectroscopy (FCS) captures these subtle dynamical changes at a single-protein level in terms of the diffusion coefficient.[15-17] The autocorrelation function of fluctuations in the signals from fluorescent molecules diffusing in and out of the focal volume allows us to determine the diffusion coefficient of a molecule and consequently its size. For example, by analyzing the diffusion coefficient of Bovine Serum Albumin (BSA) in real time, Samanta et al observed a structural transformation of BSA in dimethyl sulfoxide solution.[18] The FCS technique was further developed for such studies. On the basis of FCS and the time-correlated single-photon counting (TCSPC) technique, Enderlein et al invented the time-resolved fluorescence correlation spectroscopy in 2001.[19] TCSPC records the detection times of individual photons of several detection channels with picosecond accuracy, which contains plenty of information, such as the fluorescence correlation, fluorescence lifetime, antibunching anisotropy effects and so on.[20, 21] Taking advantage of TCSPC technique, we can track structural transitions of proteins by means of the fluorescence lifetime as well as the diffusion coefficient. In order to obtain steady and reliable fluorescence signals, commercially available fluorescence dyes are usually used to label the target protein in FCS experiments.[22-24] In our present work, we label BSA with a fluorescence dye ATTO-488 to obtain a fluorescence probe ATTO-BSA. This dye

Soft Matter Accepted Manuscript

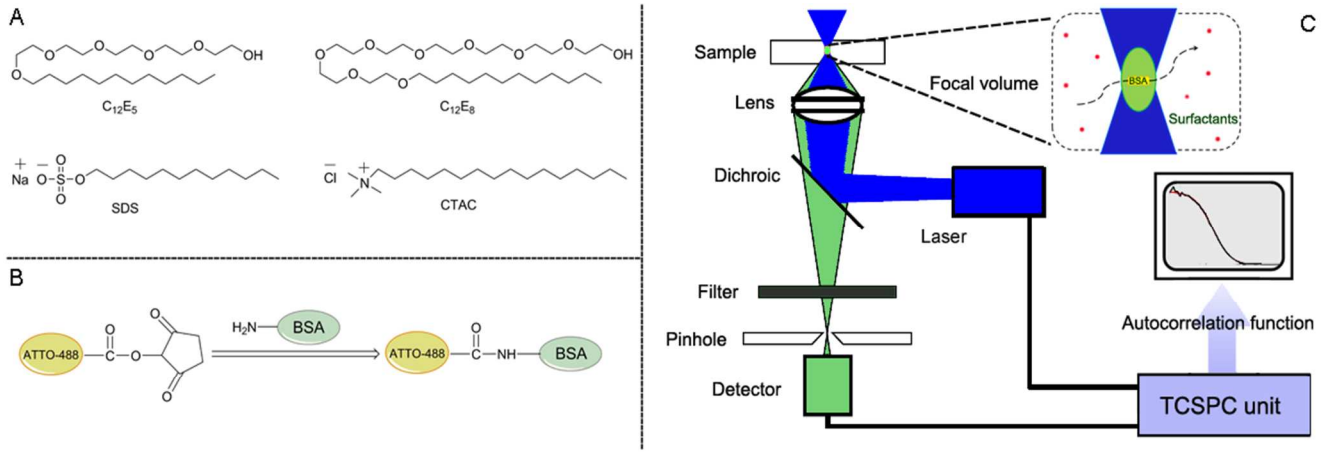

Fig. 1 (A) Chemical structures of nonionic (pentaethylene glycol monododecyl ether, $C_{12}E_5$ and octaethylene glycol monododecyl ether, $C_{12}E_8$), anionic (sodium dodecyl sulfate, SDS), and cationic (cetyltrimethylammonium chloride, CTAC) surfactants. (B) Scheme for labeling protein BSA with fluorescence dye ATTO-488. (C) FCS setup. The light from an Argon-Ion laser (488 nm) passes through a water immersion microscope objective to excite the fluorescence sample. The emitted fluorescence light is collected by the detector and further fed to TCSPC unit. The fluorescence lifetime is obtained by fitting the slope of fluorescence decay curves of photons, while the residence time by fitting the autocorrelation function of fluorescence in the focal volume.

possesses a high quantum yield (0.80) and a sufficient Stoke's shift.

Diffusion plays a key role in many aspects of biological activities of proteins in organisms.[25, 26] In this study, we employ FCS and fluorescence lifetime measurements to monitor structural changes of BSA in different (anionic, cationic and neutral) surfactant solutions by analyzing the diffusion coefficient and fluorescence lifetime of ATTO-BSA at single-protein level. Different structures of BSA in CTAC (positive), SDS (negative) $C_{12}E_5$ (neutral) and $C_{12}E_8$ (neutral) solutions as a function of concentration are observed. We distinguish whether the structural transition of BSA in these solutions is induced by micelles or surfactant monomers.

Materials and Methods

Materials

Cationic surfactant CTAC (purity: 99%) and anionic surfactant SDS (purity: 99.9%) were purchased from TCI and Roth, respectively. Nonionic surfactants $C_{12}E_5$ (purity: 99%) and $C_{12}E_8$ (purity: 99%) were purchased from Fluka. Fluorescence dyes rhodamine 110, BSA and ATTO-488 protein label kit were purchased from Sigma-Aldrich.

Labelling BSA with ATTO NHS-Ester

First, we dissolved 1 mg of BSA in 1 ml of labeling buffer (mixture of PBS buffer and 0.2 M sodium bicarbonate solution, pH 8.3). Then we dissolved 1.0 mg of ATTO-488 NHS-Ester in 50 μl of anhydrous, amine-free DMSO. Next, a three-fold molar excess of the ATTO-488 solution was added to the protein solution with gentle shaking. We incubated the reaction mixture protected from light for up to 1 hour at the room temperature. Finally, we separated the ATTO-BSA conjugate from the free dye by a gel filtration column. ATTO-488 is a small molecule which does not affect the physical and chemical properties of BSA after labelling.

Fluorescence Correlation Spectroscopy

The basis of FCS was first introduced by Elson and Magde in the early 1970s.[27-29] In FCS experiments, the distribution of the laser light intensity (I) in the focal volume is often approximated by a three dimensional Gaussian: $I(x, y, z) = I_0 \exp(-2(x^2 + y^2)/L^2 - 2z^2/H^2)$, where L is the cross sectional length in the x - y plane, and H is the height of the illuminated region of the focal volume. Fluctuations of the fluorescence intensity, $\delta F(t)$, can be analyzed by means of the autocorrelation function: $G(\tau) = \langle \delta F(t)\delta F(t+\tau)\rangle / \langle F(t)\rangle^2$, where $\delta F(t) = F(t) - \langle F\rangle$. In the case of three-dimensional isotropic single-component diffusion with the triplet state correction, $G(\tau)$ is given by[30]

$$G(\tau) = (1 + \frac{p}{1-p} e^{-\tau/\tau_t}) \frac{1}{N} \frac{1}{(1+(\frac{\tau}{\tau_i}))(1+\frac{1}{\omega^2}(\frac{\tau}{\tau_i}))^{1/2}} \quad (1)$$

where p is the fraction of dye molecules in the triplet state, τ_t is the triplet lifetime, N is the average number of molecules in the focal volume, τ_i is the residence time of a molecule in the focal volume, and $\omega = H/L$ is a structure parameter equal to the ratio of the longitudinal to transverse size of the focal volume. The residence time, τ_i, is related to the corresponding diffusion coefficient, D_i, by $D_i = L^2/(4\tau_i)$ for the transverse direction. The transverse radius of the focal volume, L, is obtained from the calibration measurement of the residence time before each experiment. First we measure the free diffusion of rhodamine 110 in water ($D_{rh110} = 4.7 \pm 0.4\times10^{-10}$ m^2s^{-1}),[31] for calibration. The typical residence time of rhodamine 110 in the focal volume, τ_{rh110}, is around 20 μs and the value of ω is about 5 in our FCS setup.

The FCS setup used in our experiments (Fig. 1 (C)) was a commercial inverted NIKON EZ-C1 confocal microscope. The focal setup was additionally equipped with PicoHarp 800 FCS setup made by PicoQuant. The experiments were conducted at 25 °C using a 488 nm Argon-Ion laser for illumination. A water immersion objective with a numerical aperture equal 1.2 and magnification of 60 was used in FCS measurements. Before each measurement a drop of filtered, de-ionized water was used as the

Soft Matter Accepted Manuscript

This journal is © The Royal Society of Chemistry [year]

immersion medium between the sample, cover-glass and the objective. During measurements the laser power was set at a constant level and the focal volume was at a constant distance of 10 μm from the edge of the cover-glass. An avalanche photo diode was used for detection. All surfactant solutions were prepared with a probe concentration of ~10^{-9} M. 200 μl of the solution was transported into the sample container (8 Chambered Coverglass-Lab-Tek®) and analyzed by FCS. Each measurement (duration 60 s) was repeated at least ten times and the autocorrelation function curves were analyzed by SymPho Time program.

The diffusion coefficient of the molecule studied, D_i, and the diffusion coefficient of rhodamine 110, D_{rh110}, are related to their residence times via[32]

$$D_i/D_{rh110} = \tau_{rh110}/\tau_i \quad (2)$$

According to the Stokes-Sutherland-Einstein equation, D_i is given by:

$$D_i = k_B T/(6\pi\eta_0 R_{h,i}) \quad (3)$$

where k_B is the Boltzmann constant, T is the absolute temperature, and η_0 is the solvent viscosity.

We combine equations (2) and (3) to calculate the hydrodynamic radius of the molecule studied, $R_{h,i}$:

$$R_{h,i} = k_B\tau_i T/(6\pi\eta_0\tau_{rh110}D_{rh110}) \quad (4)$$

Fluorescence lifetime analysis

The fluorescence lifetime of ATTO-BSA in surfactant solutions was conducted at 25 °C by using a pulsed laser. The value of fluorescence lifetime is acquired by fitting the fluorescence decay curves with a mono-exponential model according to the formula:

$$I(t) = I_0 \exp(-t/\tau) \quad (5)$$

where I_0 is the initial intensity, t is the time after the absorption, and τ is the fluorescence lifetime.

The fluorescence lifetime is a kinetic parameter determined from

$$\tau = 1/(k_r + k_{nr}) \quad (6)$$

where k_r and k_{nr} are the rate constants of the radiative process and the nonradiative process (known as quenching), respectively.[21]

Results and discussion

Diffusion and Structural properties

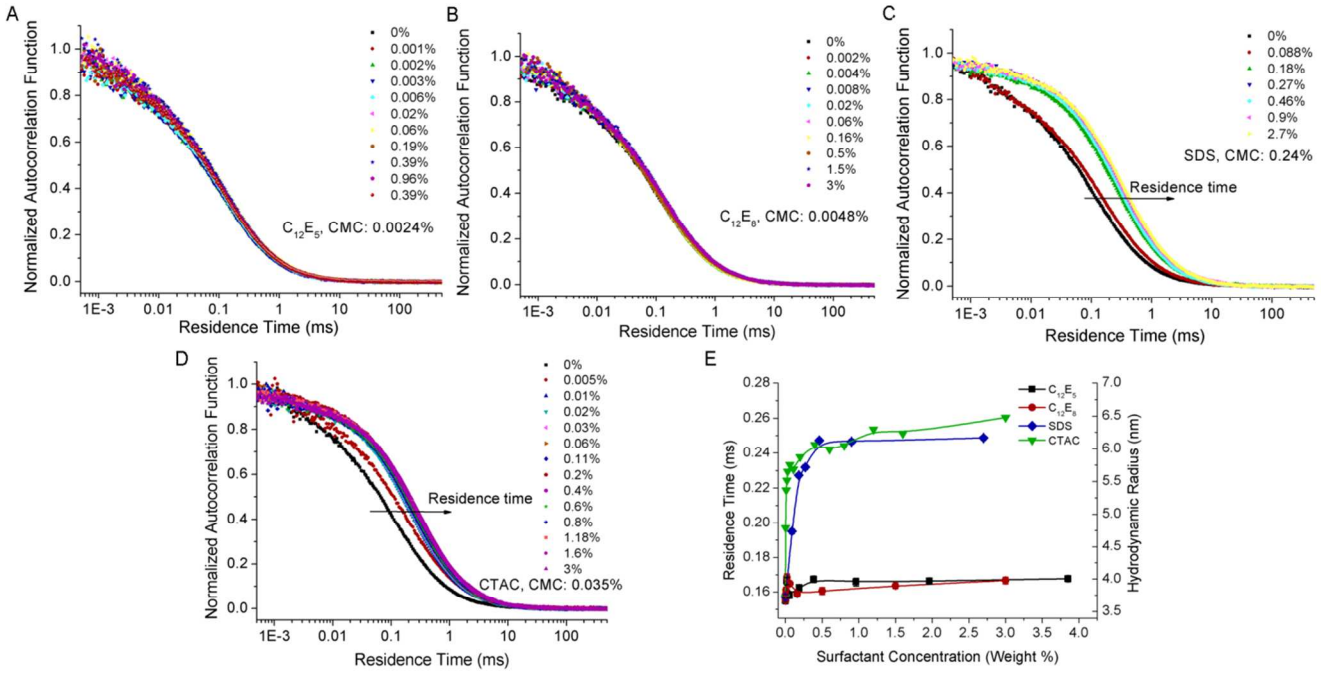

Fig. 2 (A), (B), (C) and (D) Normalized experimental autocorrelation function curves of ATTO-BSA diffusing in the solutions of $C_{12}E_5$, $C_{12}E_8$, SDS and CTAC, respectively. The overlapping sets of data points in (A) and (B) indicate that the residence time of BSA in the $C_{12}E_5$ and $C_{12}E_8$ solutions does not dependent on the surfactant concentration. In (C) and (D), a sudden increase in the residence time is found in both the SDS and CTAC solutions at concentrations below the CMC. (E) Residence time and hydrodynamic radius of BSA for the four surfactant solutions as a function of concentration. The residence time and hydrodynamic radius of the BSA in $C_{12}E_5$ or $C_{12}E_8$ solutions is roughly the same as in pure water, whereas a sudden transition is observed in the ionic surfactant solutions. Structure of BSA undergoes an apparent change in ionic surfactant solutions. Error bars are smaller than the symbols.

We use equation (1) to fit the average residence times of rhodamine 110 and BSA in the focal volume and obtain the values 0.02 and 0.15 ms, respectively. At various concentrations below or above the CMC of $C_{12}E_5$ (CMC at 0.06 mM, 0.0024%) and $C_{12}E_8$ (CMC at 0.09 mM, 0.0048%),[33] we do not observe any noticeable changes in the residence time of BSA during its diffusion in the solutions (Fig. 2 (A) and (B)). The residence time of BSA in these solutions is around 0.16 ms (see Fig. 2 (E)), and is roughly the same as in pure water. Therefore the structure of BSA is stable in nonionic surfactant solutions.[34] Our previous work on the mobility of lysozyme protein in the hexaethylene glycol monododecyl ether ($C_{12}E_6$) solution is also consistent with

Soft Matter Accepted Manuscript

the present result. The diffusion coefficient of lysozyme did not change in the $C_{12}E_6$ solution within the same range of surfactant concentration.[35]

In the case of BSA diffusing in highly diluted solutions of SDS, we observed an abrupt increase in the residence time (Figure. 2 (C)). The transition takes place at the concentration of 0.088% SDS, which is three times below CMC (0.24% at 25 °C).[36] A slight increase in the SDS concentration (to 0.18%) leads to a sudden jump of the residence time, which indicates the structure of BSA undergoes a significant change in this range of concentration. As the concentration of SDS increases up to 0.46%, the residence time of BSA approaches a constant value.

This result agrees with the classic "necklace-bead" model which attributes the structural change of the protein to the protein-surfactant interactions and binding. The model distinguishes: (I) specific binding, where only a small amount of surfactant molecules binds to the specific high-energy sites of the protein without changing its structure; (II) non-cooperative binding; (III) cooperative binding, where unfolding of protein is believed to start, and (IV) saturation, suggesting further binding of surfactant does not occur on the protein.[2] We observe that when the concentration of SDS is below 0.088%, the interaction between BSA and SDS belongs to region (I): only a small amount of SDS molecules binds to the specific high-energy site of the protein without causing its structural change. The region of saturation (above 0.18%, below CMC) is clearly seen in Fig. 2 (C) and is very close to the earlier report from the dynamic light scattering (DLS) measurement with the result of 0.21%.[4] Nevertheless, the range of regions (II) and (III) where the protein begins to unfold, from 0.088% to 0.18% in our case, is too narrow to distinguish them. A similar trend is also observed in the BSA-CTAC system (Fig. 2 (D)). The structural transition of BSA takes place at the concentration of 0.005% CTAC in solution, which is seven times smaller than the CMC (0. 035% or 1.1 mM, 25 °C).[37] BSA becomes saturated with CTAC once the concentration of CTAC reaches around 0.02% (still below CMC).

Nonionic surfactants ($C_{12}E_5$ and $C_{12}E_8$) bind to BSA through hydrophobic interactions and hydrogen bonds, however, these interactions are too weak to change the structure of BSA.[38] Instead, they prevent the protein from aggregation.[34, 39] In contrast, the electrostatic interactions between the ionic surfactants and BSA are much stronger than the hydrophobic interactions and hydrogen bonds, leading to the significantly structural changes of BSA. Therefore, the electrostatic interaction seems to be the most significant driving force for the structural change of BSA.[40]

Zirwer et al proposed an empirical equation: $R_h = (2.8 \pm 0.3)\, N_a^{0.5 \pm 0.02}$ (in angstroms), to predict the hydrodynamic radius of a highly unfolded protein, where N_a denotes the number of amino acid residues in a single polypeptide chain.[41] The hydrodynamic radius of unfolded BSA (N_a = 583) is 6.8 ± 0.7 nm according to the empirical equation. Using the diffusion coefficient of rhodamine 110 (D_{rh110} = 4.7 ± 0.4×10^{-10} m^2s^{-1}), we calculate the hydrodynamic radius of BSA in surfactant solutions via equation (4). The calculated hydrodynamic radius of BSA after the structural transition is 6.2 nm (Fig. 2(E)), close to the published result of 6.0 nm by DLS.[4] The calculated radius of BSA-CTAC complex is 6.5 nm, which is slightly bigger than that of BSA-SDS complex.

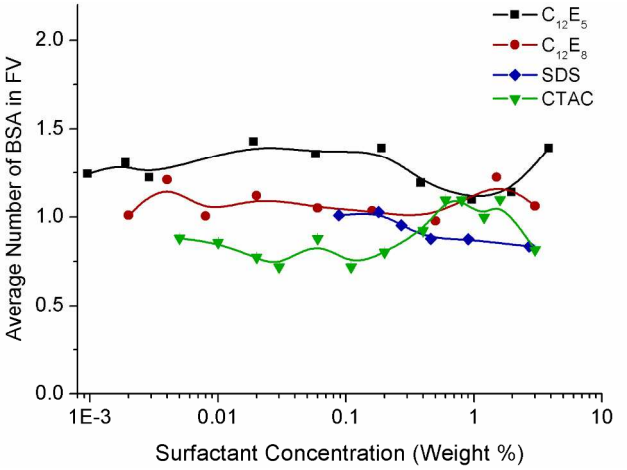

Fig. 3 The average number of ATTO-BSA (*N*) diffusing through the focal volume in $C_{12}E_5$, $C_{12}E_8$, SDS and CTAC solutions as a function of surfactant concentration. Error bars are smaller than the symbols.

In some cases the increase in the hydrodynamic radius results from the self-aggregation of proteins. However, it happens only when the protein concentration is high enough.[18] In our experiment, we did not observe such a phenomenon because of the extremely low concentration of BSA in surfactant solutions. We compared the average numbers of BSA molecules staying in the focal volume in each BSA-surfactant system by fitting the autocorrelation function curves with equation (1). The values of *N* does not change as a function of surfactant concentration (Fig. 3), excluding aggregation of BSA. Slight fluctuation of *N* in each system may result from high sensitivity of FCS technique, which requires the probe concentration of ~10^{-9} M only. Riekkola group proved that BSA did not aggregate in the presence of SDS.[40]

There is still no consensus on the cause of the structural transitions of proteins in surfactant solutions.[9] From the results obtained from SDS and CTAC, we conclude that BSA experiences a sudden structural transition in ionic surfactant solutions at a concentration far below CMC, where only surfactant monomers are present. Thus, the structural transition of BSA is caused by ionic surfactant monomers.

Fluorescence lifetime properties

The fluorescence lifetime of a fluorophore is determined by its chemical structure and shape.[42] It is also affected by the external nanoenvironment and molecular interactions.[21] To confirm the structural transition of BSA caused by the protein-surfactant interaction, we have investigated the fluorescence lifetime of ATTO-BSA in the four surfactant solutions by FCS. We found that the fluorescence decay curves of ATTO-BSA in nonionic surfactant $C_{12}E_5$ and $C_{12}E_8$ solutions with varying concentration do not change (Fig. 4 (A) and (B)). The value of the fluorescence lifetime fitted to equation (5) is 2.36 ns and does not depend on the surfactant concentration. In contrast, a sudden increase in the fluorescence lifetime of ATTO-BSA is observed in the ionic surfactant solutions (Fig. 4 (C) and (D)). It increases by 28%, from 2.36 to 3.0 ns, in SDS solution with the transition concentration at 0.088% (below its CMC) and by 21%, from 2.36 to 2.84 ns, with the transition point at 0.005% (below its CMC) in

Soft Matter Accepted Manuscript

This journal is © The Royal Society of Chemistry [year]

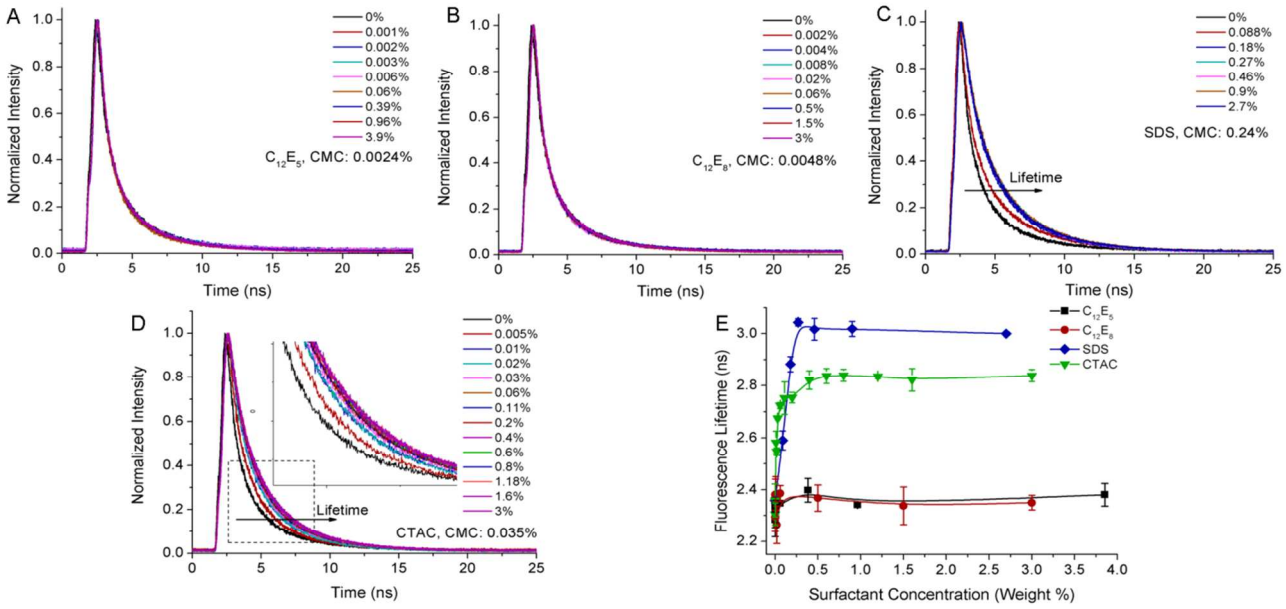

Fig. 4 (A), (B), (C) and (D) Fluorescence decay curves of ATTO-BSA in $C_{12}E_5$, $C_{12}E_8$, SDS and CTAC solutions with varying concentration. The overlapping curves in (A) and (B) suggest a constant fluorescence lifetime of ATTO-BSA in $C_{12}E_5$ and $C_{12}E_8$ solutions, while left-shifted curves in (C) and (D) indicate the lifetime transition of the probe in SDS and CTAC solutions below their CMC; (E) illustrates the average fitted values of the fluorescence lifetimes of ATTO-BSA in $C_{12}E_5$, $C_{12}E_8$, SDS and CTAC solutions as a function of concentration according to equation (5). The lifetime of the probe in $C_{12}E_5$ or $C_{12}E_8$ solutions is the same as in pure water, however, sudden jumps are observed in ionic surfactant solution.

CTAC solution. In both cases this change occurs at the same concentration as observed in the residence time in FCS experiment.

The increased fluorescence lifetime of ATTO-BSA in ionic surfactant solutions indicates different nanoenvironments of ATTO-488, which is caused by either BSA or surfactant solutions. In order to find out which of them really causes the lifetime transition of ATTO-488, we measured the fluorescence lifetime of free ATTO-488 in these surfactant solutions. We found that the fluorescence decay curves of ATTO-488 in the four surfactant solutions with selected concentrations displayed a same trend (Fig 5 (A)). The fitted value of the fluorescence lifetime is 4.17 ns, close to the reported result (4.1 ns) by Kapusta.[43] In contrast, the lifetime of ATTO-488 decreases by as much as 44%, to 2.36 ns, after binding to BSA (Fig 5 (B)). It can be concluded that the fluorescence lifetime of ATTO-488 was influenced only by BSA but not by the surfactant solutions.

Based on the results above, we attribute the fluorescence lifetime transition of ATTO-BSA in ionic surfactant solutions to the structural change of BSA. According to equation (6), the sum of rate constant of radiative and nonradiative process, $k_{nr} + k_{nr}$, is inversely proportional to the average fluorescence lifetime. The unfolding of BSA reduces its quenching effect to the dye, leading to the decrease in k_{nr} and raise of the lifetime. Therefore, the fluorescence lifetime of ATTO-488 increases suddenly after the structural transition of BSA. This point of view gets support from the work of Lober's group. They found that the lifetime of dye 8-ANS labeled to the bovine carbonic anhydrase B and human α-lactalbumin significantly increases after the proteins are denatured by guanidinium chloride.[44] In contrast, the nonradiative process in ATTO-BSA is not influenced by nonionic surfactant solutions at all due to the unchanged structure of BSA. As a

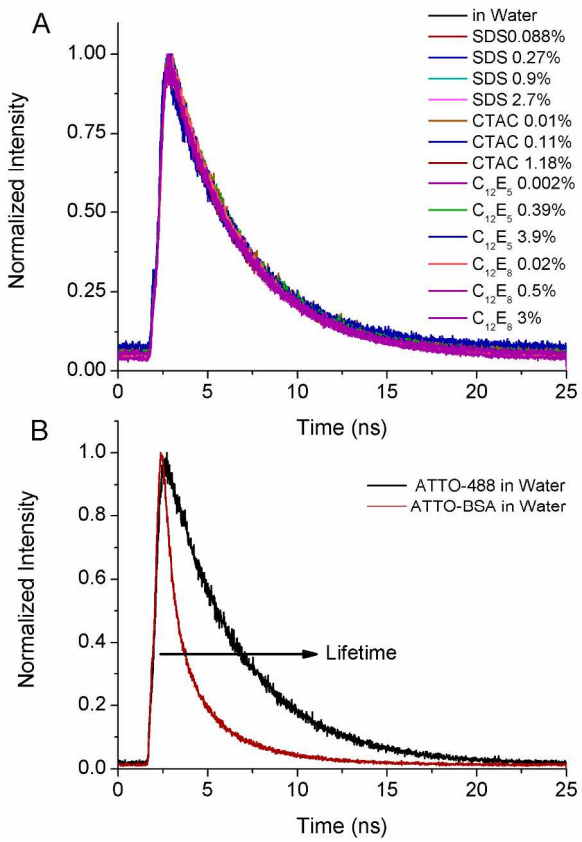

Fig. 5 (A) Fluorescence decay curves of dye ATTO-488 in $C_{12}E_5$, $C_{12}E_8$, SDS and CTAC solutions with selected concentrations. The overlapping curves suggest few changes in lifetime of ATTO-488 in the four surfactant solutions. (B) Fluorescence decay curves of dye ATTO-488 and ATTO-BSA in water. A dramatically decrease in fluorescence lifetimes of ATTO-488 is observed after labeling to BSA.

Soft Matter Accepted Manuscript

consequence, the fluorescence lifetime of the probe in nonionic surfactant solutions stays constant.

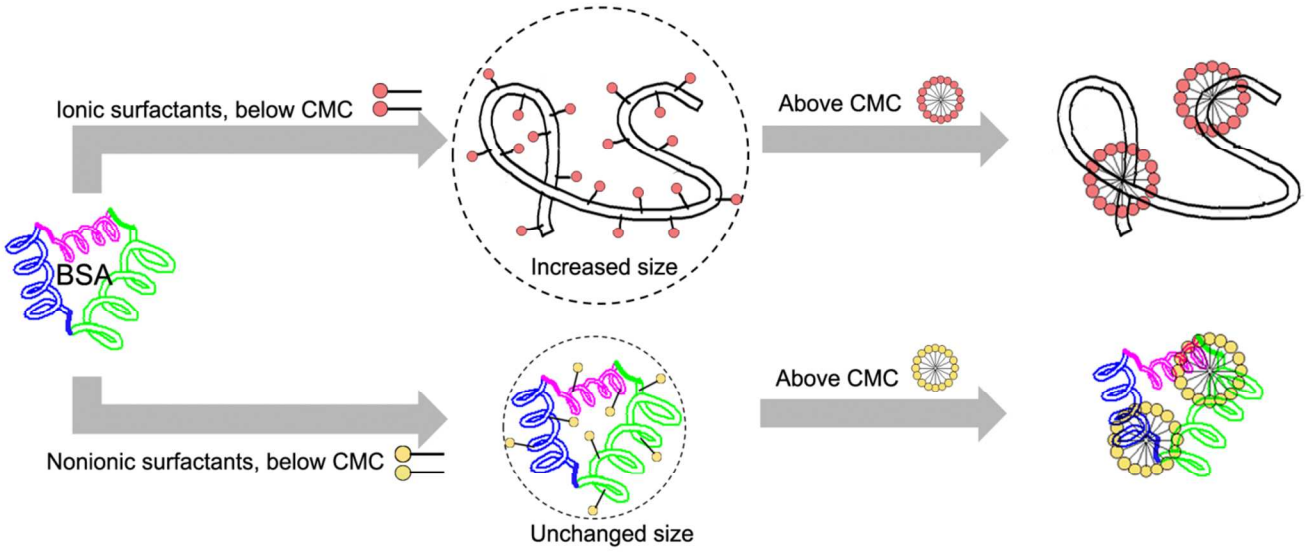

Fig. 6 Suggested mechanism of the structural changes of BSA in ionic surfactant solutions with the concentration below and above CMC.

Noticeably, the structural transition of BSA in ionic surfactant solutions obtained from the fluorescence lifetime measurements coincides with the results from FCS. It is evident that the structural transition is induced by ionic surfactant monomers but not micelles, with the transition concentration far below CMC (Fig. 6). The hydrodynamic radius and fluorescence lifetime of ATTO-BSA before and after the structural transitions are summarized in Table.1.

Table 1 Comparison of hydrodynamic radius (R_h) and fluorescence lifetime (τ) of ATTO-BSA in water and surfactant solutions

	R_h (nm)	τ(ns)
Without structural change		
Water	3.88 ± 0.029	2.36 ± 0.064
$C_{12}E_5$	3.99± 0.11	2.34 ± 0.041
$C_{12}E_8$	4.01 ± 0.092 (3.79)[a]	2.34 ± 0.044
With structural transition		
SDS (2.7%)	6.16 ± 0.029 (5.9)[a]	3.02 ± 0.028
CTAC (3.0%)	6.52 ± 0.037	2.84 ± 0.023

[a] Reference values from dynamic light scattering experiment from ref 2

Conclusion

We have studied the diffusion and structural properties of BSA in four surfactant solutions ($C_{12}E_5$, $C_{12}E_8$, CTAC and SDS) by FCS technique. We observe structural transitions of BSA in diluted SDS and CTAC solutions at concentrations well below CMC, with the calculated hydrodynamic radius at 6.2 and 6.5 nm in respective. In contrast, the globular BSA does not change its structure at all in $C_{12}E_5$ and $C_{12}E_8$ solutions. Its hydrodynamic radius is still 3.9 nm as in pure water.

We confirm the structural transition of BSA by the fluorescence lifetime results. The lifetime of ATTO-BSA increases suddenly from 2.36 ns in water to 3.02 ns in SDS solutions and to 2.84 ns in CTAC solutions. However, no change in the fluorescence lifetime is observed in nonionic surfactant solutions. We have found that the structural transition of BSA in highly diluted ionic surfactant solutions is far below their CMC, thus the structural transition of BSA is induced by surfactant monomers, not micelles.

Acknowledgements

This work was supported by the grant from National Science Centre granted on the basis of decision number 2011/02/A/ST3/00143 (Maestro grant). This work was done using the equipment from the NanoFun laboratories founded by POIG.02.02.00-00-025/09.

Notes and references

Institute of Physical Chemistry, PAS, Kasprzaka 44/52, 01-224 Warsaw, Poland. E-mail: rholyst@ichf.edu.pl.

1. S. Ghosh, *Colloid Surface A*, 2005, **264**, 6-16.
2. N. J. Turro, X. G. Lei, K. P. Ananthapadmanabhan and M. Aronson, *Langmuir*, 1995, **11**, 2525-2533.
3. S. Ghosh, *Colloid Surface B*, 2008, **66**, 178-186.
4. A. Valstar, M. Almgren, W. Brown and M. Vasilescu, *Langmuir*, 2000, **16**, 922-927.
5. K. K. Andersen, C. L. Oliveira, K. L. Larsen, F. M. Poulsen, T. H. Callisen, P. Westh, J. S. Pedersen and D. Otzen, *J Mol Biol*, 2009, **391**, 207-226.
6. S. F. Santos, D. Zanette, H. Fischer and R. Itri, *J Colloid Interf Sci*, 2003, **262**, 400-408.
7. X. H. Guo, N. M. Zhao, S. H. Chen and J. Teixeira, *Biopolymers*, 1990, **29**, 335-346.
8. M. N. Jones, *Chem Soc Rev*, 1992, **21**, 127-136.
9. D. Otzen, *Bba-Proteins Proteom*, 2011, **1814**, 562-591.
10. X. H. Guo and S. H. Chen, *Chem Phys*, 1990, **149**, 129-139.
11. Shiraham.K, K. Tsujii and T. Takagi, *J Biochem*, 1974, **75**, 309-319.
12. A. Chakraborty, D. Seth, P. Setua and N. Sarkar, *J Phys Chem B*, 2006, **110**, 16607-16617.
13. T. Chakraborty, I. Chakraborty, S. P. Moulik and S. Ghosh, *Langmuir*, 2009, **25**, 3062-3074.
14. H. Yang, G. B. Luo, P. Karnchanaphanurach, T. M. Louie, I. Rech, S. Cova, L. Y. Xun and X. S. Xie, *Science*, 2003, **302**, 262-266.
15. E. L. Elson, *Traffic*, 2001, **2**, 789-796.
16. K. Bacia and P. Schwille, *Methods*, 2003, **29**, 74-85.

Soft Matter Accepted Manuscript

This journal is © The Royal Society of Chemistry [year]

17. S. T. Hess, S. H. Huang, A. A. Heikal and W. W. Webb, *Biochemistry*, 2002, **41**, 697-705.
18. A. Pabbathi, S. Patra and A. Samanta, *Chemphyschem*, 2013, **14**, 2441-2449.
19. M. Bohmer, M. Wahl, H. J. Rahn, R. Erdmann and J. Enderlein, *Chem Phys Lett*, 2002, **353**, 439-445.
20. H. Yang and X. S. Xie, *J Chem Phys*, 2002, **117**, 10965-10979.
21. M. Y. Berezin and S. Achilefu, *Chem Rev*, 2010, **110**, 2641-2684.
22. K. Chattopadhyay, S. Saffarian, E. L. Elson and C. Frieden, *P Natl Acad Sci USA*, 2002, **99**, 14171-14176.
23. J. Szymanski, A. Patkowski, A. Wilk, P. Garstecki and R. Holyst, *J Phys Chem B*, 2006, **110**, 25593-25597.
24. T. Kalwarczyk, N. Ziebacz, A. Bielejewska, E. Zaboklicka, K. Koynov, J. Szymanski, A. Wilk, A. Patkowski, J. Gapinski, H. J. Butt and R. Holyst, *Nano Lett*, 2011, **11**, 2157-2163.
25. Y. Q. Wang, C. G. Li and G. J. Pielak, *Journal of the American Chemical Society*, 2010, **132**, 9392-9397.
26. M. Weiss, H. Hashimoto and T. Nilsson, *Biophysical Journal*, 2003, **84**, 4043-4052.
27. D. Magde, W. W. Webb and E. Elson, *Phys Rev Lett*, 1972, **29**, 705-&.
28. E. L. Elson and D. Magde, *Biopolymers*, 1974, **13**, 1-27.
29. D. Magde, E. L. Elson and W. W. Webb, *Biopolymers*, 1974, **13**, 29-61.
30. O. Krichevsky and G. Bonnet, *Rep Prog Phys*, 2002, **65**, 251-297.
31. P. O. Gendron, F. Avaltroni and K. J. Wilkinson, *J Fluoresc*, 2008, **18**, 1093-1101.
32. R. Holyst, A. Bielejewska, J. Szymanski, A. Wilk, A. Patkowski, J. Gapinski, A. Zywocinski, T. Kalwarczyk, E. Kalwarczyk, M. Tabaka, N. Ziebacz and S. A. Wieczorek, *Phys Chem Chem Phys*, 2009, **11**, 9025-9032.
33. G. Olofsson, *J Phys Chem-Us*, 1985, **89**, 1473-1477.
34. F. Donate, A. Artigues, L. Iriarte and M. Martinez-Carrion, *Protein Sci*, 1998, **7**, 1811-1820.
35. J. Szymanski, A. Patkowski, J. Gapinski, A. Wilk and R. Holyst, *J Phys Chem B*, 2006, **110**, 7367-7373.
36. E. Dutkiewicz and A. Jakubowska, *Colloid Polym Sci*, 2002, **280**, 1009-1014.
37. L. T. Okano, F. H. Quina and O. A. El Seoud, *Langmuir*, 2000, **16**, 3119-3123.
38. M. Wahlgren, J. Kedstrom and T. Arnebrant, *J Disper Sci Technol*, 1997, **18**, 449-458.
39. N. B. Bam, J. L. Cleland and T. W. Randolph, *Biotechnol Progr*, 1996, **12**, 801-809.
40. G. Yohannes, S. K. Wiedmer, M. Elomaa, M. Jussila, V. Aseyev and M. L. Riekkola, *Anal Chim Acta*, 2010, **675**, 191-198.
41. G. Damaschun, H. Damaschun, K. Gast and D. Zirwer, *Biochemistry-Moscow+*, 1998, **63**, 259-275.
42. Y. E. Chen and A. Periasamy, *Microsc Res Techniq*, 2004, **63**, 72-80.
43. P. Kapusta, R. Machan, A. Benda and M. Hof, *Int J Mol Sci*, 2012, **13**, 12890-12910.
44. V. N. Uversky, S. Winter and G. Lober, *Biophys Chem*, 1996, **60**, 79-88.

Soft Matter Accepted Manuscript